低エネルギー領域での
イオン・原子衝突の二重微分断面積測定

（課題番号　60540241）

昭和６１年度科学研究費補助金　　一般研究Ｃ　　研究成果報告書

昭和６２年３月

研究代表者　　伊　藤　　陽

（城西大学理学部講師）

低エネルギー領域でのイオン・原子衝突の二重微分断面積測定

（課題番号　６０５４０２４１）

昭和６１年度科学研究費補助金　　一般研究Ｃ　　研究成果報告書

昭和６２年３月

研究代表者　　伊　藤　　陽

（城西大学理学部講師）

はしがき

この報告書は、昭和６０年度・６１年度の２年間にわたって行われた文部省科学研究補助金一般研究Ｃ「低エネルギー領域でのイオン・原子衝突の二重微分断面積測定」の研究成果報告書である。

この研究で目的としたことは、実験室系エネルギー１０eV程度の領域でのイオンと原子の衝突過程の研究の為の、ビーム実験装置を建設し、衝突に関与するポテンシャル交又に関する情報を得ることである。

研究組織

研究代表者　　伊藤　陽　　(城西大学理学部講師)

研究経費

昭和６０年度	１，２００千円
昭和６１年度	５００千円
計	１，７００千円

研究発表

(1) 伊藤　陽　「低エネルギーイオン衝突実験装置の試作」
日本物理学会　第４０回年会　　昭和６０年４月１日

(2) 伊藤　陽　「希ガス２価イオン・希ガス系での一電子移行過程」
日本物理学会　第４１回年会　　昭和６１年４月１日

****

C O N T E N T S

****

I. Introduction

Differential cross sections measured for selected collision processes, which are called doubly differential cross sections, imply impact parameter dependences of transition probabilities for the processes. As more informations are included in differential cross sections than integral ones, they are often required to compare with theoretical results in detail. For example, a very interesting observation and explanation for the double-charge transfer process in $C^{4+} + He \rightarrow C^{2+} + He^{2+}$ are reported recently[1]. The experimental and theoretical results are shown in figure 1. The undulation observed in the differential cross section is interpreted as a type of Stueckelberg oscillation. From this kind of study, one could get detailed information for the process and the interaction potential of the system as well.

We aimed to construct an apparatus to measure differential cross sections for various inelastic processes, for example, charge transfer reactions or fine-structure transitions or electronic excitations or de-excitations with this proposal in Grant-in-aid for scientific reserch (1986) so as to study the mechanism and the selection rules for these processes.

We have selected slow doubly charged ion-atom collisions as a first step of the project with following reasons.

(i) Inelastic scattering processes are often induced by

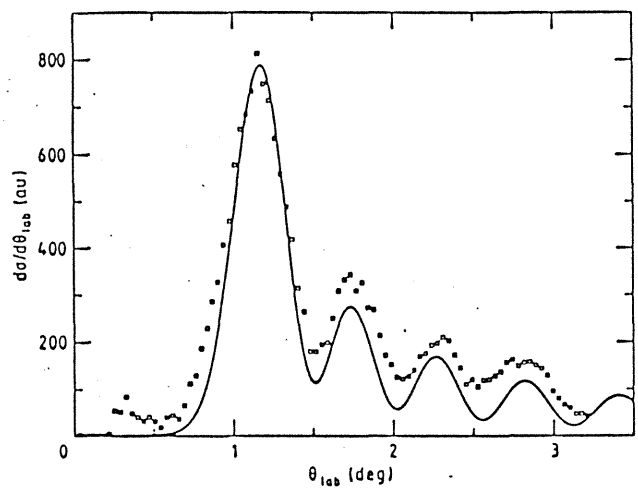

Cross section $d\sigma/d\theta_{lab}$, differential in the laboratory scattering angle θ_{lab}, as a function of the laboratory scattering angle. The semiquantal method gives the full curve while the squares represent experimental values (C L Cocke, private communication). The theoretical spectrum is folded with a Gaussian function having a standard deviation of 1.5 mrad (approximately 0.09°) corresponding to the experimental resolution. It is given in atomic units while the experimental spectrum is drawn to an arbitrary scale. The impact energy E_{lab} is 1520 eV.

figure 1; Experimental (□) and theoretical (line) cross sections in C^{4+} + He ---> C^{2+} + He^{2+} reaction at E_{lab} = 1520 eV (E_{cm} = 380 eV).

potential crossings of adiabatic electronic states. The mechanism of the transitions around these crossing points are considered to be due to radial and rotational couplings between the states[2]. At low energy region, for example below 10 eV in the laboratory frame, it may safely be assumed that the dominant mechanism is a pure radial coupling, consequently experimental results can be compared with theoretical ones comprehensively.

(ii) Theories for non-adiabatic transitions due to potential crossings are progressed considerably, however, there exists some difficulties for the application of these theories to experimental results. Generally, an acculate interaction potential is not known for a selected collision system, therefore estimations of the position of potential crossing or the coupling matrix element evaluation are difficult. For the case of doubly-charged-ion atom collisions, the dominant inelastic process at low energy region is known to be one-electron capture process [3]; such as

$$A^{++} + B \rightarrow A^{+} + B^{+} + \Delta E, \quad \text{---------} \quad (1)$$

where ΔE is the exthothermicity. The position of the crossing is easily calculated as

$$R_c\ (\text{Å}) = 14.4/\Delta E\ (\text{eV}) \quad \text{----------} \quad (2)$$

when one disregars polarization effect in the initial channel and considers Coulomb interaction only in the final channel. This assumption is normally reasonable because the crossing points exist at fairly large internuclear distance. Therefore, at least, one of the difficulties can be eliminated in this collision process. From the experimental point of view, the products in

final channel are both charged particles. They are easily to be energy-analysed and detected, therefore, detailed informations for the potential crossings can be obtained and state-selective measurements are enabled.

(iii) Though the importance of doubly differential cross section measurements is well noticed, only few measurements are reported for charge-transfer process [3] . This may be due to experimental difficulties to produce and handle low energy ion beam because of the space-charge effect or the Coulomb repulsion among the ions. We have also aimed to develop and accumulate experimental techenique in slow-ion-collision experiment with beam method.

II. Experimental

A schematic diagram of the apparatus constructed is shown in figure 2. It consists of an electron-impact ion-source, a sector type mass-selector, which is made of a Ferrite parmanent magnet, cylindrical deceleration lenses, a collision chamber or an effusive target-beam source, an electrostatic double cylindrical energy-analyser, and an ion detector. Almost all the parts are made of stainless steel (SUS 316). Mean radius of the mass-selector is 30 mm, and mean radii of sectors used as analysers are both 25 mm. The inner-diameter of the lens element is 15 mm for primary beam side and the design of the lens-system was carried according to the discription by Harting and Read[5].

Ions created by an electron-impact of about 150 eV are extracted from the source by an extraction-electrode to which potential difference of about -15 V from the ion-source was applied. With this weak extraction field, narrow energy-spread of the primary ion-beam of 0.05 X q (eV) ,(q is the charge number of the ions), was achieved without using an energy-selector. Ions were then mass selected and decelerated to desired collision energy by series of lenses and focused to the collision region. Angular width of the primary beam was about + 1 degree (FWHM) for 10 eV Ar^{++} beam. We used the same type of the ion-source reported by Nakamura et al.[5]. They measured the fraction of metastable ions included in the rare gas doubly-charged ion-beam, which was found to be a mixture of ^3P, ^1D and ^1S states with nearly a statistical ratio, 9:5:1. The beam composition used in this experiment is

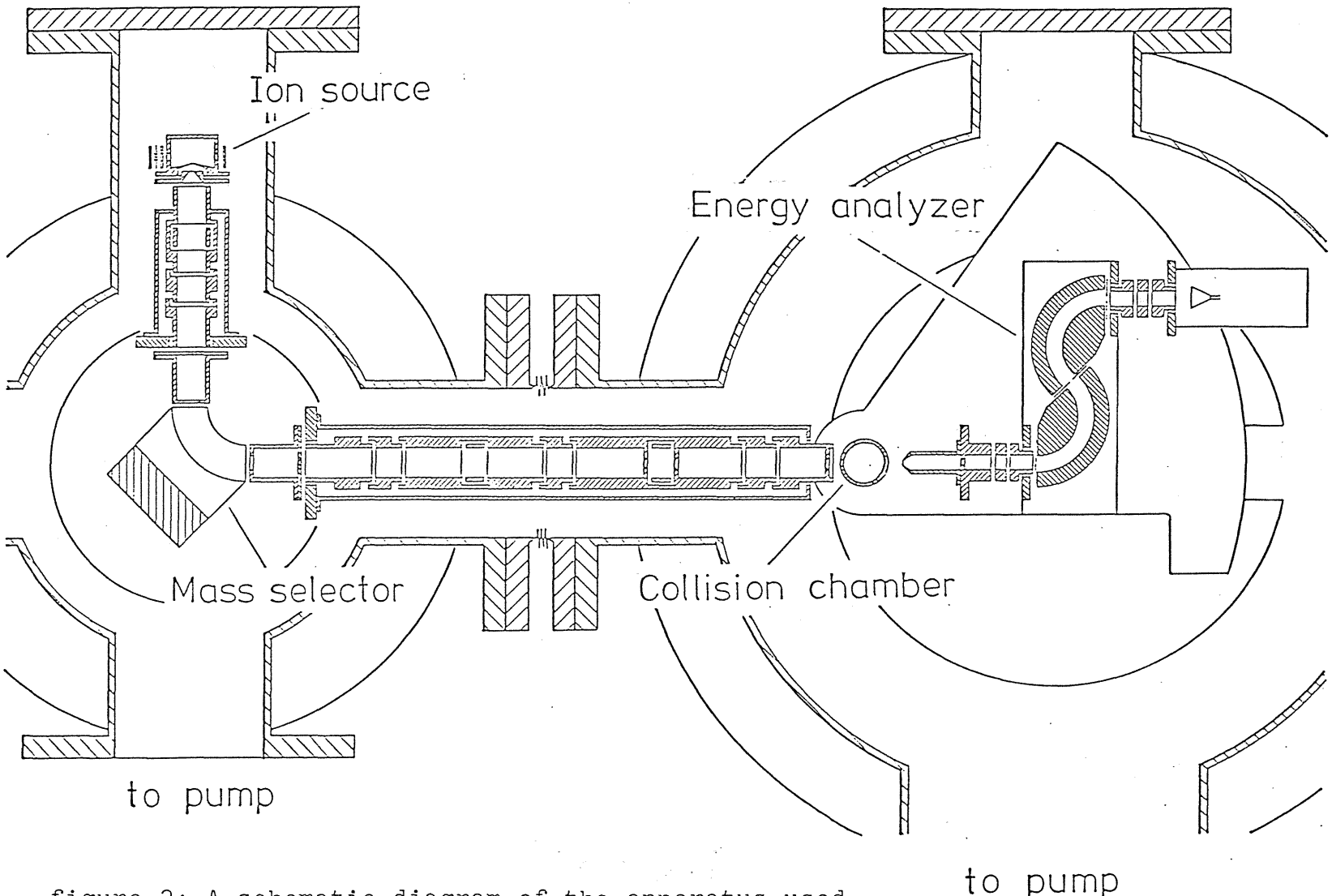

figure 2: A schematic diagram of the apparatus used.

considered to be the same as reported by Nakamura et al.. After the collisions, scattered ions were again decelerated to about 2 x q eV, which is the transmission energy of the analyser, and energy-analysed and detected by the channel-ion-detector, a Ceratron. The beam intensity of Ar^{++} at E_{lab} = 10 eV was typically 3 X 10^{-11} A and Ar^{+} about 2 X 10^{-10} A at E_{lab} = 5 eV. Whole system is enclosed in a vacuum chamber of which ultimate vacuum is 8 X 10^{-8} Torr.

The ion energy measured in laboratory frame is converted to exothermicity ΔE in center of mass system with following relation:

$$\Delta E = (1 + \gamma) E_f + (\gamma - 1) E_i - 2\gamma\sqrt{E_f E_i} \cos\theta \quad \text{----- (3)}$$

where γ is the mass ratio of the projectile, M_A, to that of the target, M_B. E_i and E_f indicate the ion-energy before and after the collision in lab. frame, respectively, and θ is the scattering angle of the projectile ion in lab. frame.

To determine the collision energy accurately, the elastic scattering in Ar^{+} - He system was measured setting the detector at 0 degree angle. A typical spectrum is shown in figure 3. As the projectile Ar^{+} ion is 10 times heavier than the target, elastically scattered Ar^{+} ions of which scattering angle of 0° and 180° are both measured at 0° in lab. frame, and the energy difference for both channels can be calculated and measured exactly. With this method, the calibration of transmission energy

of the analyser and the determination of kinetic energy of primary ion-beam were able to be carried at the same time. The accuracy of the collision energy determination in lab. system is better than ± 0.1 eV at present. The energy resolution of the analyser was about 50 meV (FWHM).

These datum were measured using a home-made multi-channel-scaler which was controlled by a micro-computer. A block diagram of the system is shown in figure 4. Control programs for measurements are mostly written in BASIC and partly in assembler. The processing speed is not fast but enough for the present purpose. The minimum voltage step to sweep ion energy is 10 mV for ± 50 V range, and 1 mV for ± 5 V range. The accuracy of the voltage step was proved to be exact with digital multi-meter.

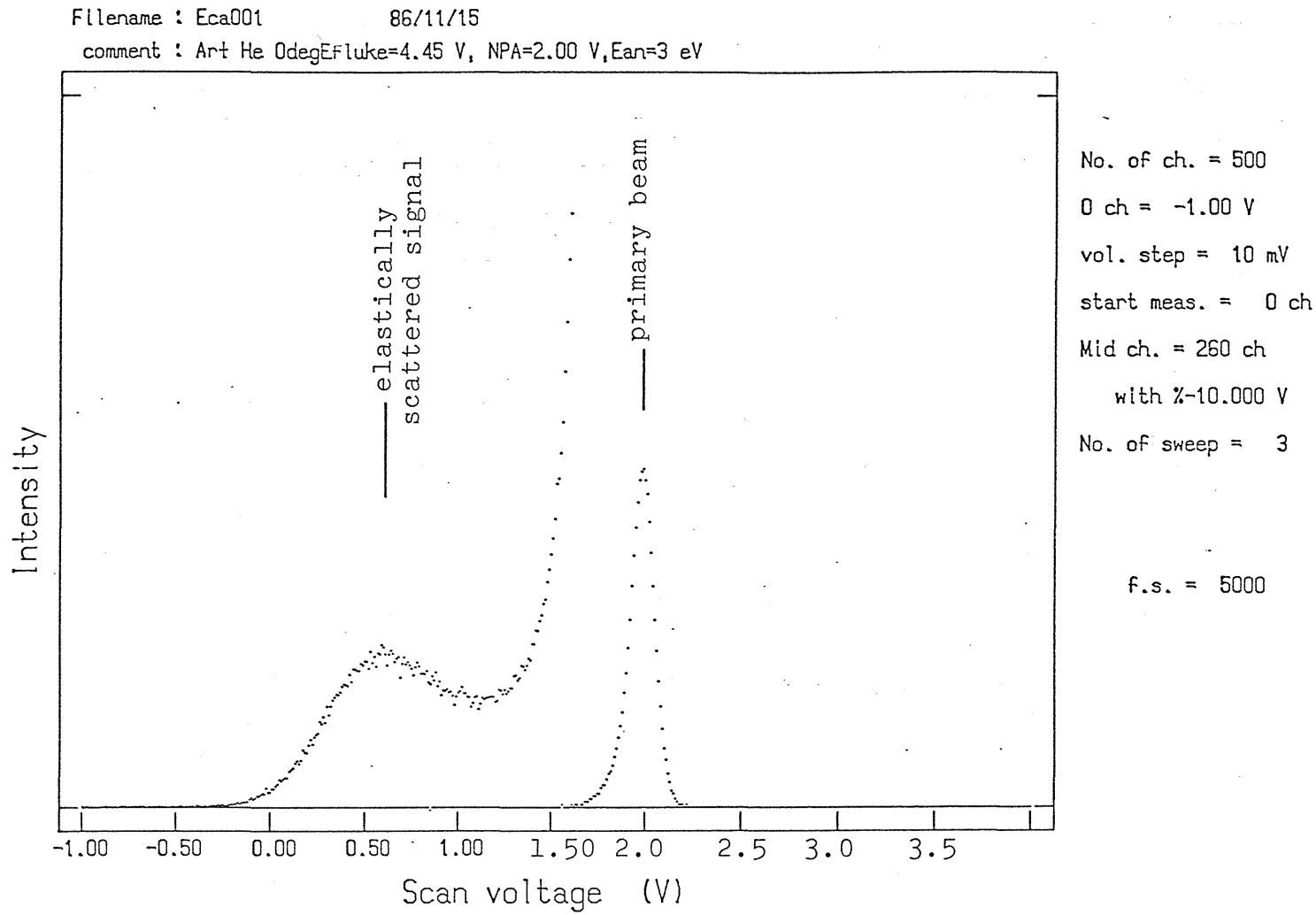

figure 3: A typical example of the ion spectrum in Ar^+ - He system for the calibration of the apparatus.

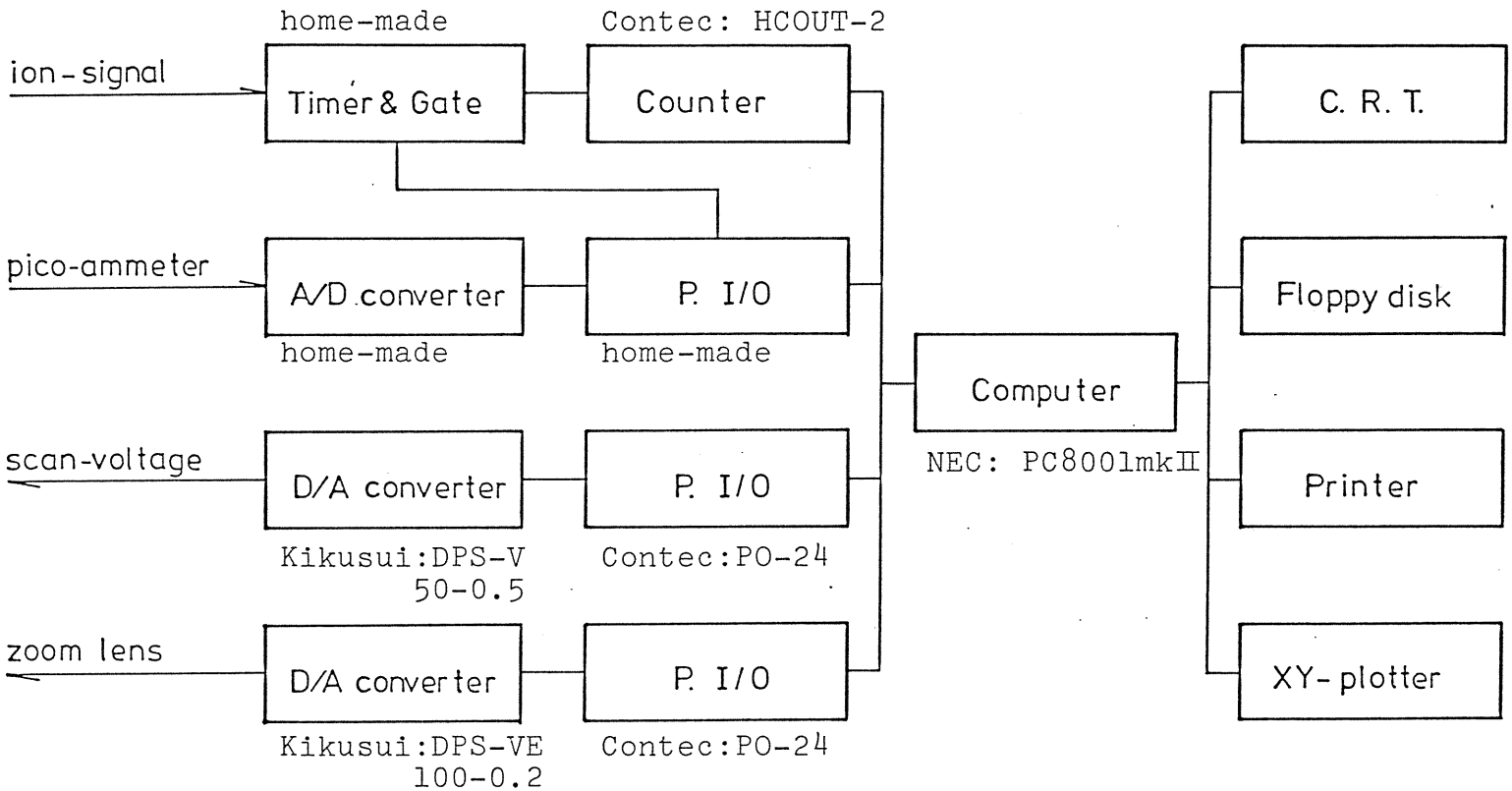

figure 4: A block diagram of the measuring system.

III. Results and discussions

III-1. One electron capture process and de-excitation of low lying metastable state in Ar^{++} - He and Kr^{++} - He system

In figure 5, a typical example of ion spectrum measured for Ar^{++} - He system is shown. The collision energy is 10 eV in lab. system, which corresponds to E_{cm} = 0.91 eV. In this collision energy, only exothermic processes, except fine-structure transitions among different J states inside of ^3P_J states of Ar^{++}, are energetically possible. As no mass-analyser was used, both Ar^+ and Ar^{++} signals are recorded in the spectrum. As We measured relative differential cross sections at $\theta_{lab} = 0^\circ$ and $\theta_{lab} = 3^\circ$, peaks indicated as (c) are normalized to unity. In the figure, the assignments of measured peaks are also indicated. From the figure, ^3P and ^1D states are seen to contribute to one electron capture process, but ^1S does not, that is,

$$Ar^{++}(^3P) + He \dashrightarrow Ar^+(^2P) + He^+(^2S) + 3.04 \text{ eV} \quad \text{----- (4)}$$

and

$$Ar^{++}(^1D) + He \dashrightarrow Ar^+(^2P) + He^+(^2S) + 4.78 \text{ eV} \quad \text{----- (5)}$$

are the dominant processes. Relative intensity ratios of the process (4) and (5), disregarding the metastable ion composition in the ion beam used, are 0.29 for $\theta_{lab} = 0^\circ$ and 0.44 for $\theta_{lab} = 3^\circ$. This means that the angular distribution of the scattered ions correspond to the process with larger exothermicity, (5), is broader than the process (4). General tendency observed in this

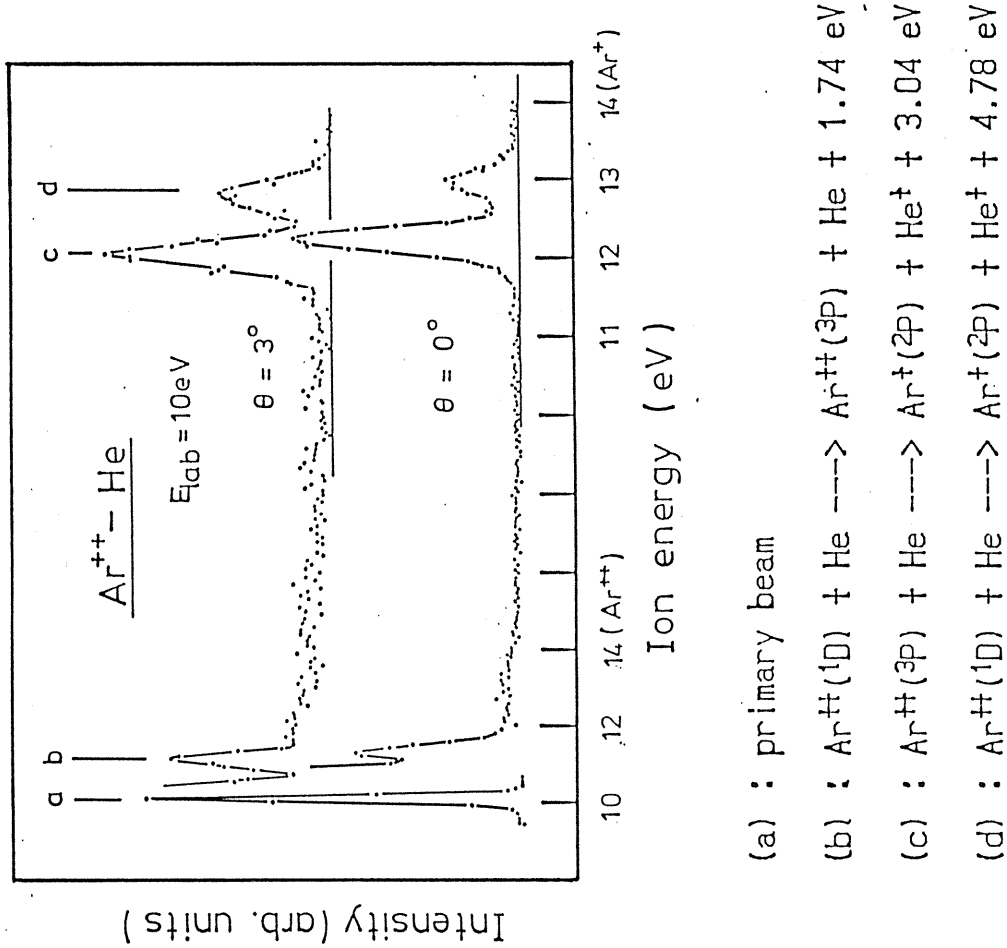

figure 5: An example of the doubly differential cross section measurements in Ar^{++} – He system at E_{lab} = 10 eV.

experiment agree well with the results reported by Friedrich and Herman for Ar^{++} - He system[3].

An adiabatic potential diagram for the system is shown in figure 6. According to the eq.(2), the position of crossing points can be calculated as R_{c4} = 4.74 Å for the process (4), and R_{c5} = 3.01 Å for the process (5). The crossing points for initial ^1S state of Ar^{++} is 2.0 Å. The broader angular distribution for the process (5) may be due to the scattering caused by stronger Coulomb repulsion effect after passing throgh the crossing point. That is, as R_{c5} locates at a smaller nuclear distance than R_{c4}, therefore, the Ar^+ ion created from $Ar^{++}(^1D)$ will be repelled stronger than that from $Ar^{++}(^3P)$.

The other peak indicated as (b) is a very typical feature observed only in Ar^{++} - He system sofar for forward scattering. This corresponds to the de-excitation process of low-lying metastable state ^1D to the ground state,

$$Ar^{++}(^1D) + He \longrightarrow Ar^{++}(^3P) + He + 1.74\ eV \quad \text{----- (6)}.$$

As the initial channel is constructed from singlet states and the final state is a mixture of singlet state and triplet state, the process (6) is a so-called spin-non-conservative collision. At higher collision energy region, it is reported that the cross section for this kind of process is in the order of 10^{-16} cm^2 [6]. No measurement is reported for the evidence of spin-non-conservative collisions at this low energy region.

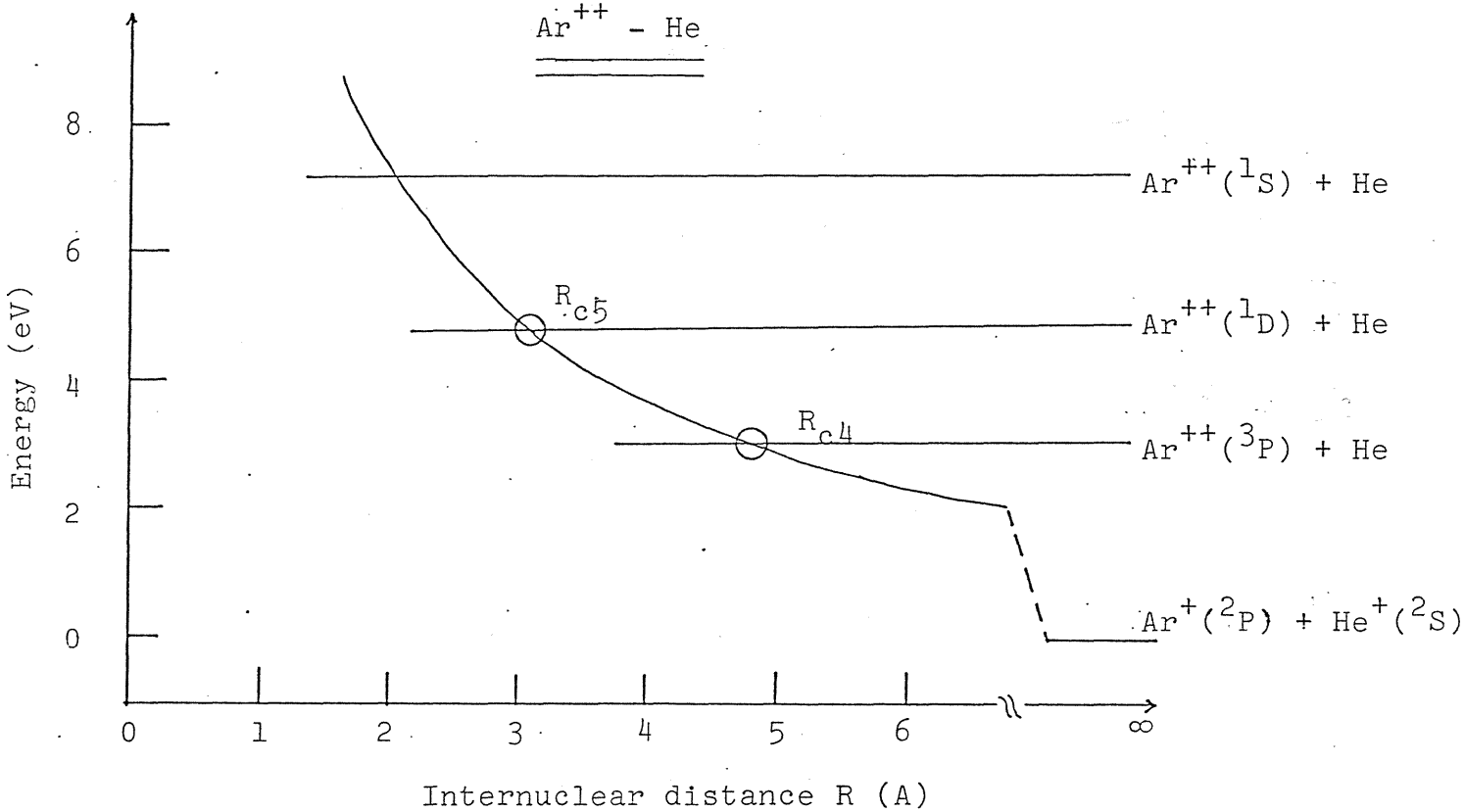

figure 6: An illustration of adiabatic interaction-potential curves in Ar^{++} - He.

In figure 7 shown is a typical spectrum obtained in Kr^{++} - He system at E_{lab} = 10 eV (E_{cm} = 0.45 eV) . The observation angle is 0 degree. In the primary beam, again ions of ^3P, ^1D, and ^1S states are included. Only a charge transfer process from ^1S state is observed, that is,

$$Kr^{++}(^1S) + He \longrightarrow Kr^{+}(^2P_{3/2}) + He^{+} + 4.08\ eV \quad ----(7),$$

and

$$\longrightarrow Kr^{+}(^2P_{1/2}) + He^{+} + 3.41\ eV \quad ----(8).$$

As the energy resolution was not sufficient, these two processes were not resolved clearly. A potential diagram for the system is shown in figure 8. The position of the crossing points are 3.53 Å and 4.22 Å.

From the comparison of Ar^{++} - He and Kr^{++} - He collisions at the same labratory collision energy, we can summarize the experimental results as follows:

(i) When the crossing points locate between 3 - 5 Å of nuclear distance, then the transition probabilities come to large. This is recently often said as a reaction window[7].

(ii) When a metastable state cotributes to charge-transfer then this state may be de-excited at the second crossing point, if the transition probability is large enough, by a backward charge-transfer process to trace the reaction path:

$$Ar^{++}(^1D) + He \longrightarrow Ar^{+}(^2P) + He^{+}(^2S)$$

$$\xrightarrow{R_{c5}}$$

$$\longrightarrow Ar^{++}(^3P) + He + 1.74\ eV. \quad ---- (6')$$

$$\xrightarrow{R_{c4}}$$

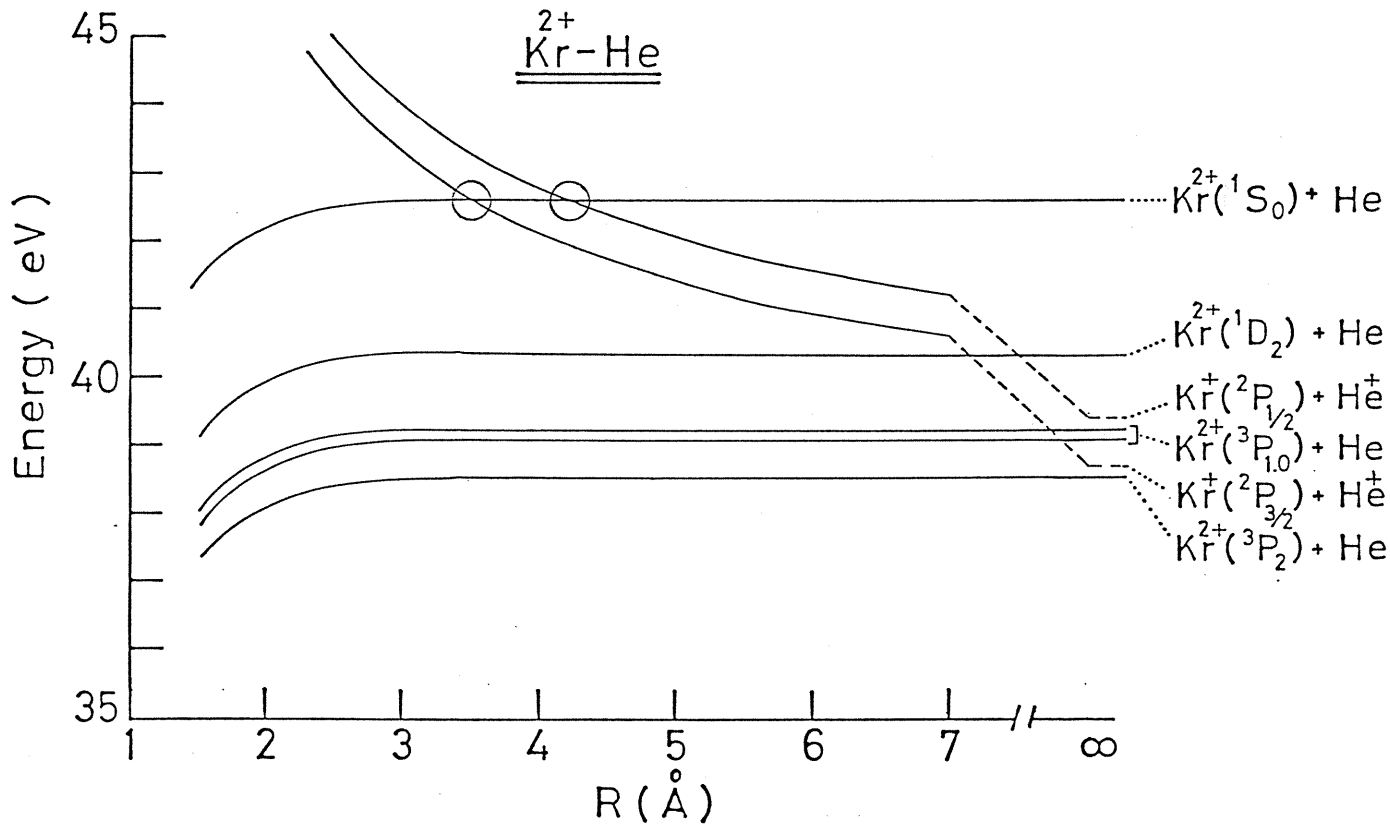

figure 8: An illustration of the interaction potential in Kr^{++} - He system.

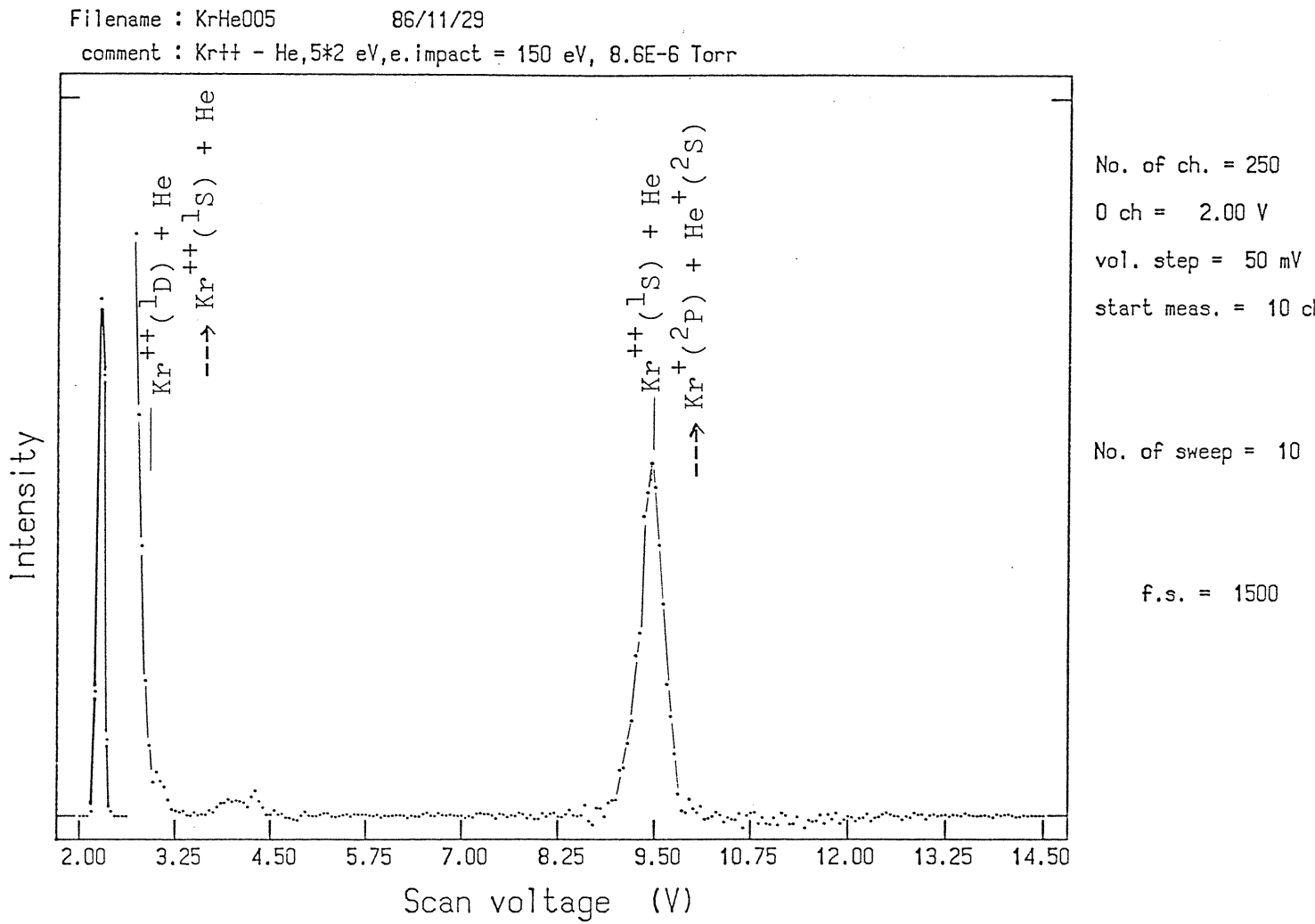

figure 7: A result of the ion spectrum obtained in Kr^{++} - He system.

A schematic illustration of the quasi molecular states constructed during the collision in Ar^{++} - He system[8] is shown in figure 9. As discussed above, in the initial channel of process (6), both the projectile ion and the target are singlet state, ^1D and ^1S, only singlet molecular states are formed. In the final channel, from the ^3P and ^1S states, $^3\Sigma$, and $^3\pi$ states are formed. According to the following selection rules predicted in radial coupling mechanism:

(i) an axial component of electron-angular momentum consevation, that is $\Sigma \to \Sigma$ and $\Sigma \nrightarrow \pi$,

(ii) a reflection symmetry conservation, $\Sigma^+ \to \Sigma^+$ and $\Sigma^+ \nrightarrow \Sigma^-$,

(iii) a spin conservation, $^1\Sigma \to {}^1\Sigma$ and $^1\Sigma \nrightarrow {}^3\Sigma$,

allowed transition points are indicated in the figure with circles. For charge transfer processes, one can find reaction pathes with keeping these selection rules shown above. However, it is im possible for the de-excitation of ^1D state because of the spin-consevation rule.

Moore has investigated the spin-non-conservative collisions in N^+ on rare gas system[9] and concluded that when the targets are changed in the order of Ar, Kr, and Xe, then the degree of the process increases at E_{lab} = 2.7 keV. In our case the tendency is fully reversed. It is only in Ar^{++} case not in Kr^{++} case that the spin non-conservative de-excitation process was observed. Therefore, the two-step mechanism (6') must be considered for our case.

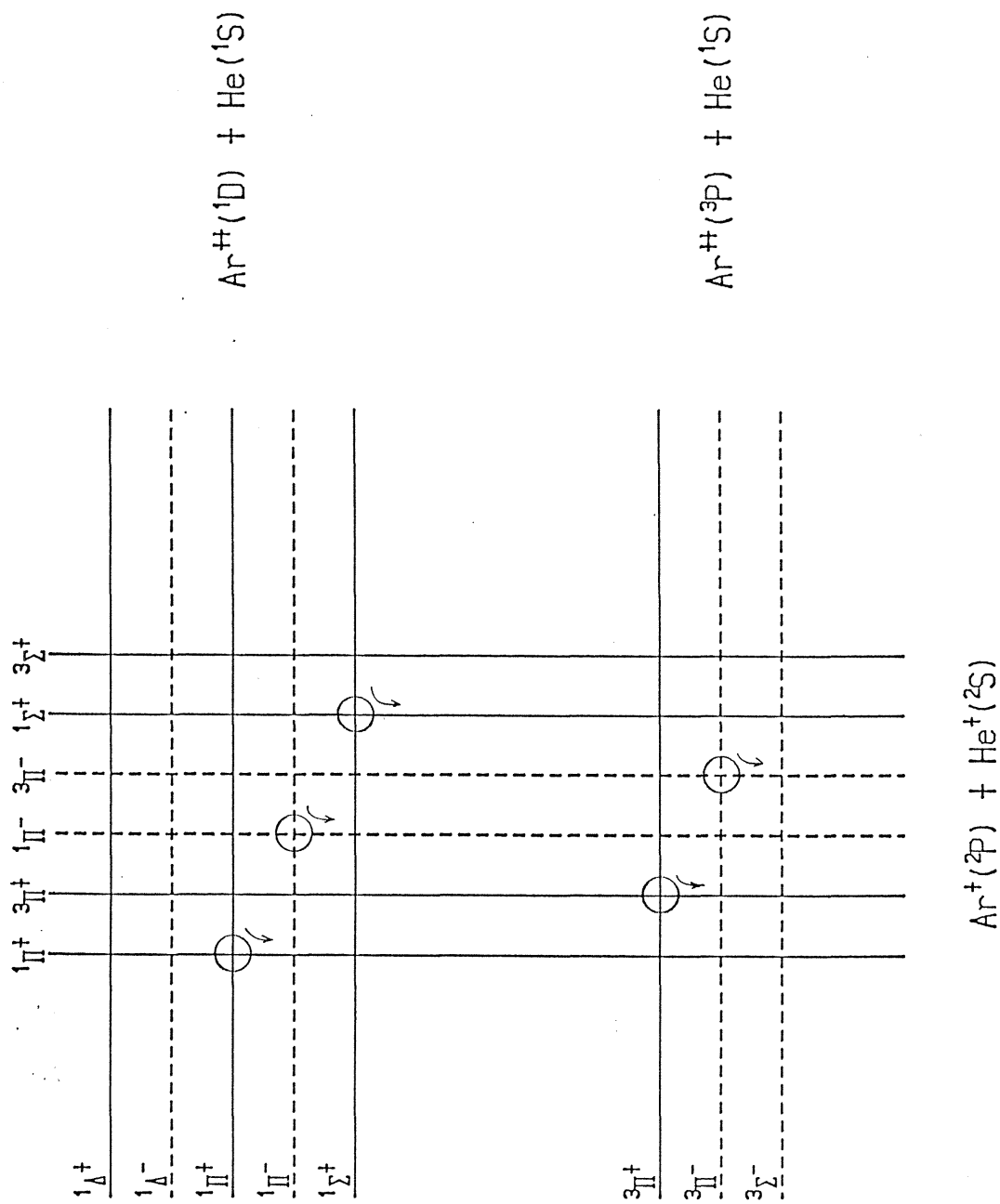

figure 9: An illustration of the quasi molecular states formed during the collision in Ar^{++} - He. Allowed transition points are indicated by circles.

A possible mechanism was found by Koike[10] theoretically to trace the reaction path for this de-excitation process without breaking the selection rules of radial coupling mechanism. According to the theory, one assume a spin-flip inside of Ar^+ itself by LS-coupling between the trajectry of the crossing points R_{c5} and R_{c4}. For the case of singlet state after the charge transfer, a change of the state may be illustrated as follows.

	Ar^+		He^+		
	m_l	m_s	m_l	m_s	
R_{c5}	0	↓	0	↑	$^1\Sigma$
↓	LS-coupling				↓
R_{c4}	1	↑	0	↑	$^3\Pi$

Then the $^1\Sigma$ state formed just after the charge-transfer at R_{c5} may be no more pure $^1\Sigma$ state but a mixture of $^1\Sigma$ and $^3\Pi$ states before reaching to second crossing point R_{c4}. Therefore at the second crossing point, one can find reaction paths for backward charge-transfer channels. With the same mechanism, the $^1\Pi$ state formed at Rc4 will change to be a mixture of $^3\Sigma$ and $^3\Pi$ states. A completion of the reaction paths are illustrated in figure 10. Detailed comparison with the theory and experiment are now in progress in numelically.

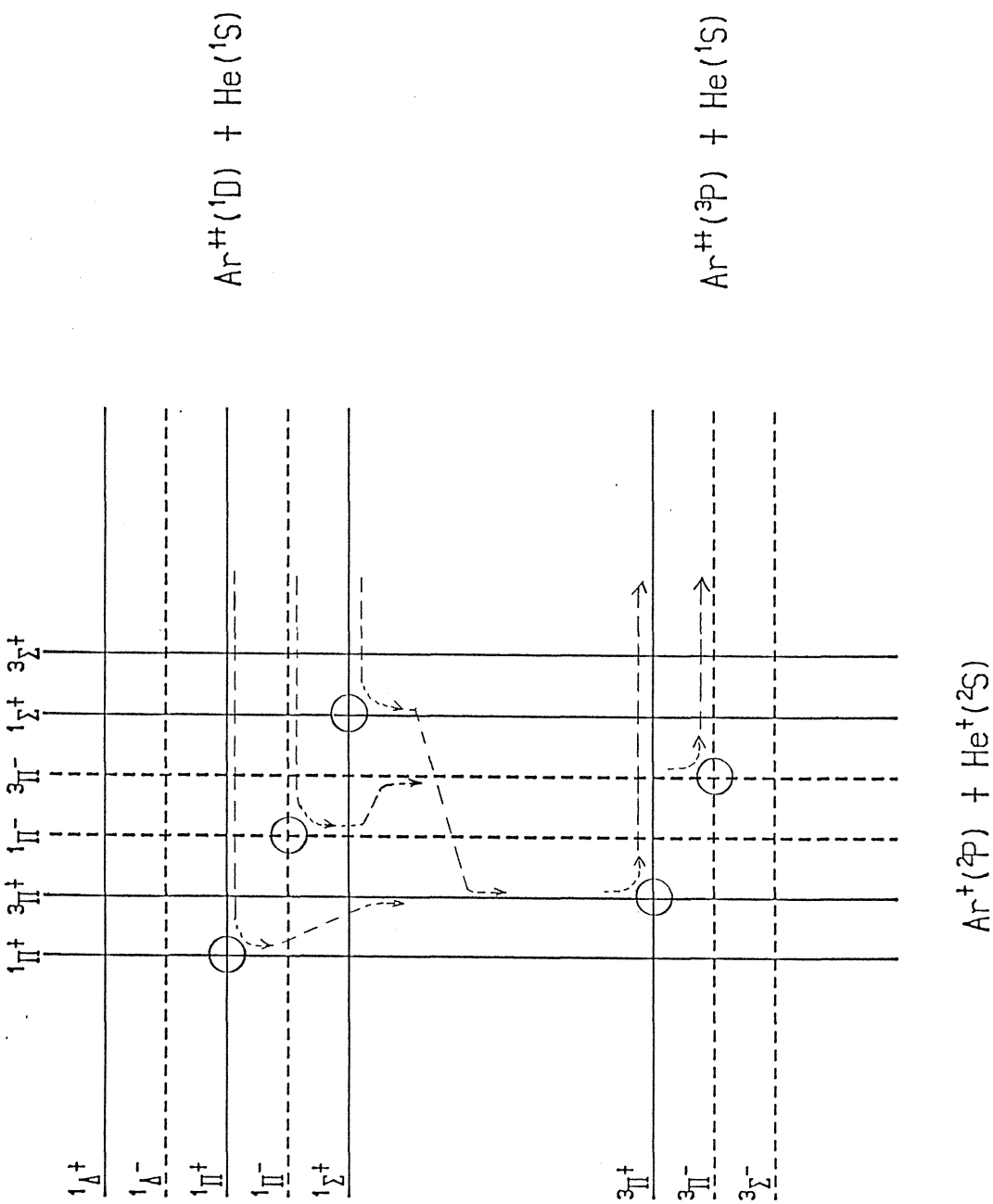

figure 10: Theoretically possible reaction paths for the de-excitation process of ^1D state in Ar^{++} - He.

III-2. Differential cross section measurements in Kr^{++} - Ne system for one-electron capture process

We have extended the measurements for other collision system. Here, we report some results obtained in Kr^{++} - Ne system for one-electron capture process.

Measured doubly differential cross sections at E_{lab} = 20 eV (E_{cm} = 3.8 eV) are shown in figure 11. Horizontal axis in this figure shows converted exothermicity in C. M. system. As we have measured only relative differential cross sections, a maximum position of each spectrum is normalized to unity. In the spectra obtained at $\theta_{lab} = 0^{\circ}$ and 2° , only two components labeled as (a) and (b) are observed. For the case of Kr^{++} - Ne case, we have taken into account the fine-structures of Kr^{++} and Kr^{+} because the energy differences of these states can not be neglected.

The peak (a) corresponds to the reaction

$$Kr^{++}(^3P_2) + Ne \longrightarrow Kr^{+}(^2P_{3/2}) + Ne^{+} + 2.95\ eV \quad \text{-------(9)}$$

or

$$Kr^{++}(^3P_{0,1}) + Ne \longrightarrow Kr^{+}(^2P_{1/2}) + Ne^{+} + 2.90\ eV \quad \text{-----(9')},$$

and peak (b) to

$$Kr^{++}(^3P_{0,1}) + Ne \longrightarrow Kr^{+}(^2P_{3/2}) + Ne^{+} + 3.60\ eV \quad \text{-----(10)}.$$

When the scattering angle are increased the other structures come to be seen. They are labeled as (c) and (d) which correspond to

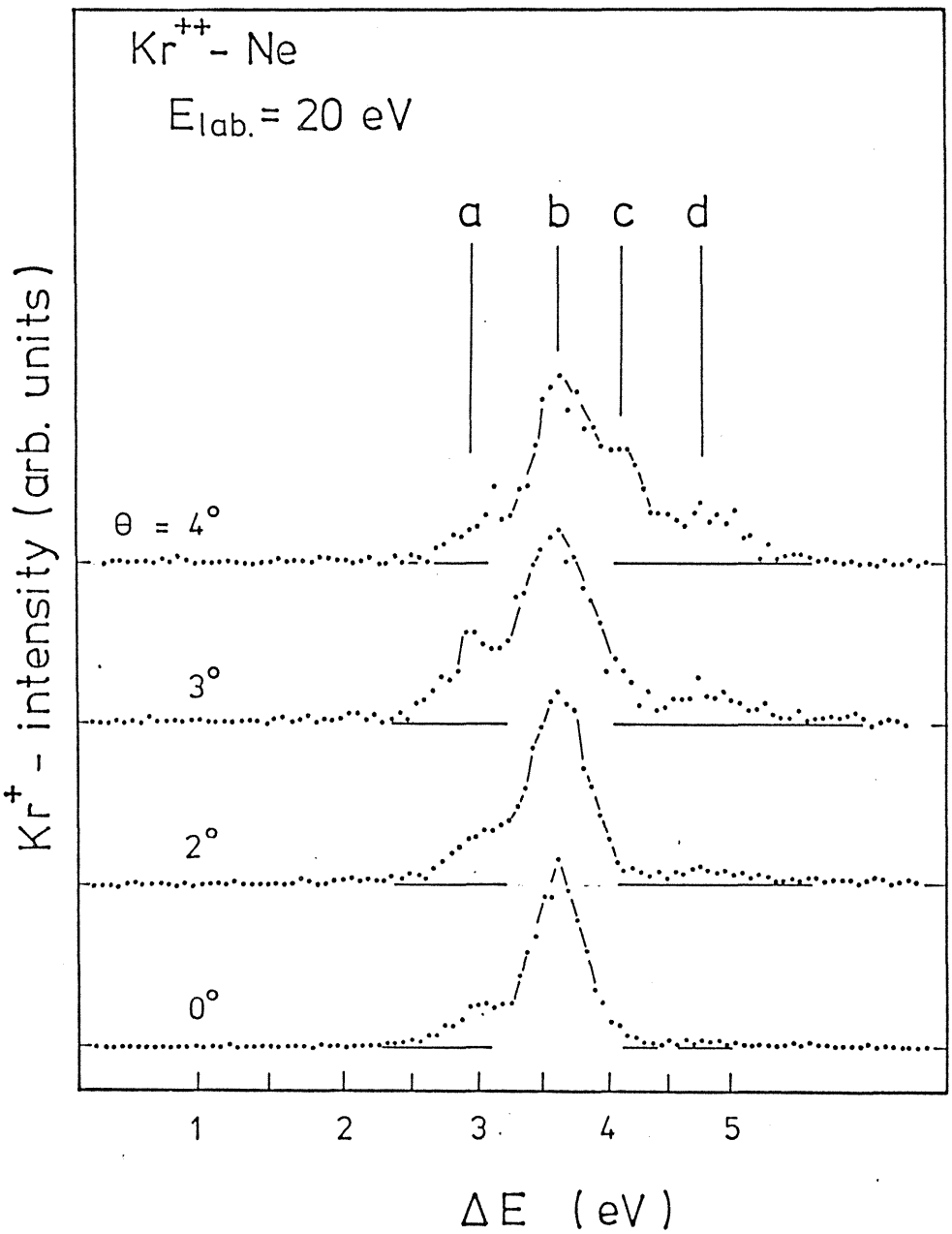

figure 11: Doubly differential cross sections measured for one-electron capture process in Kr^{++} - Ne system at E_{lab} = 20 eV.

$$Kr^{++}(^1D_2) + Ne \longrightarrow Kr^{+}(^2P_{1/2}) + Ne^{+} + 4.10\ eV \quad \text{-----(11)}$$

and

$$Kr^{++}(^1D_2) + Ne \longrightarrow Kr^{+}(^2P_{3/2}) + Ne^{+} + 4.77\ eV \quad \text{-----(12)},$$

respectively.

From these measurements, we can conclude that for smaller angle region, only the ground state, ^3P, contribute to the one-electron capture processes and with the increase of scattering angle the relative importance of metastable state, ^1D, increases. It can be seen that other metastable state, ^1S, does not at least within the angle range studied. In figure 12, interaction potentials for the system are shown, and the crossing points correspond to the reactions are shown by circles. We can understand again that when the crossing points locate within the reaction window, internuclear distance between 3 to 5 Å, the transition probability is large. Crossing points for $Kr^{++}(^1S_0)$ - He are 2.0 and 2.3 Å, which locate out of the window, consequently the cross section is negligibly small. For the reaction with larger exothermicity, the angular distribution is again seen to be broader.

Total cross section measurements for the system were carried by Koizumi et al.[11] usig a drift-tube technique in the energy range between 0.15 eV to 2 eV. In this energy range, they report that the cross sections for $Kr^{++}(^1D)$ state are about 2 - 7 times larger than that for $Kr^{++}(^3P)$. From our differential cross section measurement, at a little bit higher energy region for

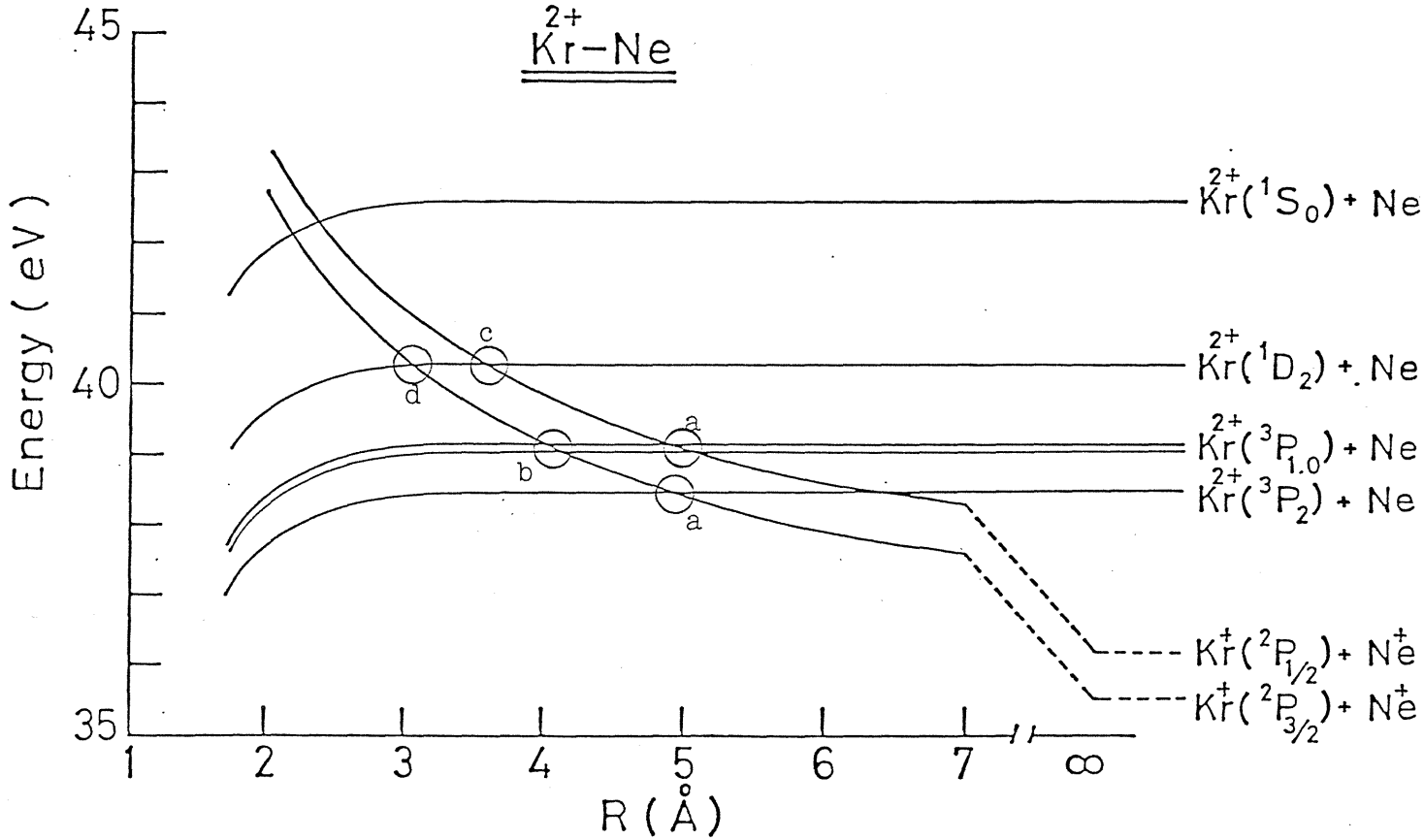

figure 12: An illustration of interaction potentials in Kr^{++} - Ne. The crossing points which correspond to one-electron capture processes are indicated by circles.

small scattering angle, main electronic state which contributes for one-electron capture process is seen to be ^3P. As the relative importance of ^1D state is observed to increase with the increase of scattering angle , then the peak height ratio of ^1D and ^3P will expected to be reversed at larger scattering angles. We may extend the measurements for a larger scattering angle.

As for a differential measurement, it took a long time to accumulate scattering signal, we have not measured acculately for the de-excitation process of ^1D in Kr^{++} - Ne system. At 0°, no signal for the de-excitation was observed. This may be reasonable because one-electron capture process from ^1D was observed at a little bit larger angle region. As at low energy collisions, such de-excitation process is considered to be due to the two step potential crossing mechanism, the signal for de-excitation process may be observed at larger scattering region. The transition path is expected to be the same as Ar^{++} - He case, that is

$$Kr^{++}(^1D) + Ne \longrightarrow Kr^{+}(^2P) + Ne^{+}(^2P)$$

$$\longrightarrow Kr^{++}(^3P) + Ne + 1.82\ eV \quad ----- \quad (13).$$

We will continue to measure for these transitions also in the future.

IV. Summary

We have constructed and tested an apparatus for low energy ion-atom collisions. An economical micro-computer controlled measuring system was also developed.

As a first step of the project, we measured one-electron capture processes for doubly-charged rare gas ion and rare gas systems. From the measurements, it is understood that

(i) the existance of reaction window at low collision energy,

(ii) the de-excitation processes of low lying metastable state must be considered for the collision systems. The process will be a conpetition process with a charge transfer reaction. We may expect from the observation to stimulate further theoretical work for selection rules when the spin-states must be considered.

(iii) The different angular distribution for the process with various exothermicity may be due to the degree of Coulomb repulsion after charge transfer reaction .

In our apparatus, a collision chamber or an effusive beam-source are used, therefore the energy resolution is mainly limited by the thermal motion of targets. To obtain more detailed information from experiments, one has to use a super-sonic nozzle-beam as a target to eliminate the thermal motion of the target atoms, and improve the energy-analyser as well.

Acknowledgement

I would like to thank Prof. I. Kanomata in Josai Univ. for his encouragement during the course of the study. I also thank Dr. F. Koike in Kitasato Univ. for sending of theoretical results correspond to de-excitation mechanism perior to publication.

References

(1) H. Danared and A. Barany: J. Phys. B19 (1986) 3109.

(2) J. B. Delos: Rev. Mod. Phys. 53 (1981) 287.

(3) B. Friedrich and Z. Herman: Chem. Phys. Lett. 107 (1984) 375.

(4) E. Harting and Read: "Electrostatic Lenses" (Amsterdam, Elsevier 1976).

(5) T. Nakamura, N. Kobayashi and Y. Kaneko: J. Phys. Soc. Jpn. 54 (1985) 2774.

(6) N. Kobayashi, T. Nakamura and Y. Kaneko: J. Phys. Soc. Jpn. 52 (1983) 2684.

(7) K. Taulbjerg: J. Phys. B19 (1986) L367.

(8) B. Hird and S. P. Ali: J. Phys. B14 (1981) 267.

(9) J. H. Moore,Jr.: Phys. Rev. A10 (1974) 724.

(10) F. Koike: private communication.

(11) T. Koizumi, K. Okuno and Y. Kanako: J. Phys. Soc. Jpn. 53 (1984) 567.